Adhesion detachment and movement of gold nanoclusters induced by dynamic atomic force microscopy

2008 J. Phys.: Condens. Matter 20 354011

(http://iopscience.iop.org/0953-8984/20/35/354011)

J. Phys.: Condens. Matter **20** (2008) 354011 (6pp) doi:10.1088/0953-8984/20/35/354011

Adhesion detachment and movement of gold nanoclusters induced by dynamic atomic force microscopy

G Paolicelli[1,4], K Mougin[2], A Vanossi[3] and S Valeri[3]

[1] CNR-INFM National Research Center S3, Via Campi 213/A, 41100 Modena, Italy
[2] ICSI–CNRS–UPR 9069 15, Rue Jean Starcky BP 2488-68057 Mulhouse Cedex, France
[3] CNR-INFM National Research Center S3 and Department of Physics, University of Modena and Reggio Emilia, Via Campi 213/A, 41100 Modena, Italy

E-mail: paolicelli.guido@unimore.it

Received 1 February 2008, in final form 6 March 2008
Published 11 August 2008
Online at stacks.iop.org/JPhysCM/20/354011

Abstract
Via dissipation processes in dynamic atomic force microscopy (AFM), we have investigated adhesion and frictional properties of deposited nanoclusters, under controlled ambient conditions. Specifically, we have considered gold nanoclusters with nominal diameters of 13 and 24 nm physisorbed on silicon substrate. The manipulation experiment has shown unambiguously that the amplitude modulation AFM method and the calibration procedure adopted allow us to discern and measure the size dependence of the energy detachment threshold for deposited objects down to the nanometer scale. Moreover, allowing us to switch easily and with high repeatability between imaging and manipulation during the AFM scans, this operational method proves to be a promising tool for inducing controlled spatial displacements at these length scales.

(Some figures in this article are in colour only in the electronic version)

1. Introduction

Experimental tests of fundamental mechanical properties at nanoscale and atomic levels have gained significant advances in the last 10–15 years thanks to the success of the AFM microscope [1–9]. In parallel, the AFM technique has been used as a versatile tool for the control and manipulation of nano-objects on surfaces [10–12]. These two fields of investigation are indeed closely correlated and it is sometimes difficult to distinguish between a step forward in the direction of fundamental understanding at the atomic scale and the advances in the AFM technique as a tool for the control and the local modification of surfaces. The technological interest in this area is also relevant because the realization of processes and devices involving nanometer size components is becoming a common issue in numerous advanced technologies.

The number of possible applications is very large, in particular for gold nanoclusters. For example, they are ideal electrodes for molecular electronics [13] and, if deposited onto thin metal oxides, they exhibit unexpectedly strong catalytic activity for different reactions, from combustion to hydrogenation and reduction [14, 15]. Finally, coated with organic molecules, these nano-objects can be used for DNA assays in genomics [16, 17], as signal amplifiers for biological recognition in biological assays.

The processes leading to the realization and optimization of these technologies are challenging. They require a joint description of both the mechanical and the chemical properties of substrates and nanoclusters taking into account that material characteristics at the nanoscale are often distinct from those of macroscale bulk solids.

The peculiar behavior of nanoclusters reflects, in general, the increasing importance of surface related properties with respect to volume material properties. This is particularly important for the understanding of adhesion and friction features of nanometer size objects and for inducing controlled movement at these length scales.

The comprehension of size dependent effects in adhesion and friction of nanoclusters on surfaces and the optimization

[4] Author to whom any correspondence should be addressed.

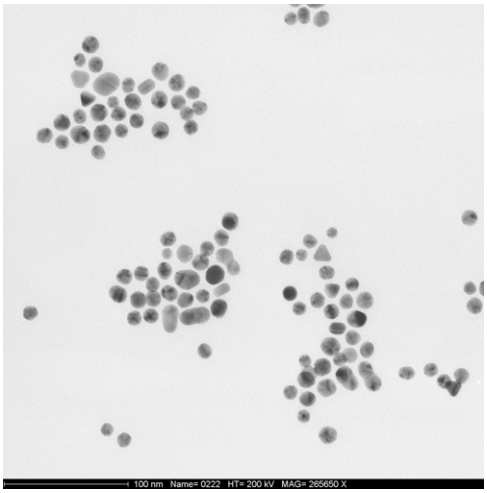

Figure 1. Typical TEM image (400 nm × 400 nm) of 13 nm diameter gold nanoclusters.

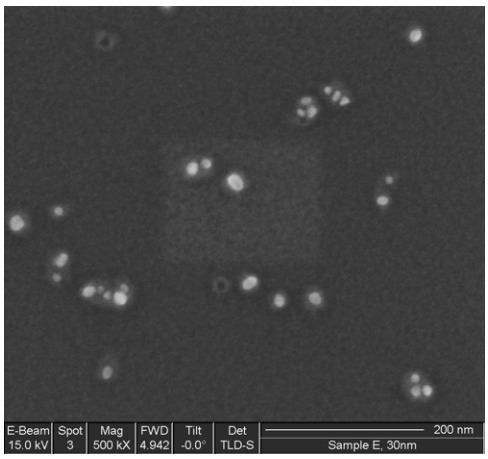

Figure 2. Typical SEM image (600 nm × 600 nm) of 13 nm diameter gold nanoclusters deposited on silicon substrate.

of a controlled procedure for manipulating them are the fundamental motivations of our experimental work.

Important results concerning the movement of individual atoms, single molecules and nanoclusters have been obtained, starting from 1990, by STM [18–21] and AFM set up in different operational ways [22, 23]. These techniques are optimized for manipulation purposes, i.e. to build up or organize controlled structures at molecular level, and not for directly measuring mechanical properties. These methods, performed in very controlled conditions, may achieve high accuracy and good repeatability in the positioning but they do not allow a careful control of the energy dissipated during the manipulation process.

A new approach has emerged during the last few years which is completely based on the control and measurement of the energy released by the AFM tip to the system when movement takes place [24–27]. The movement is induced by operating the AFM in *tapping mode* with amplitude feedback (AM-AFM) and by using a tip amplitude oscillation intentionally larger than that optimized for imaging purpose. The extra energy transferred to the cluster bound to the surface may cause its detachment and displacement. By recording the phase shift signal, when detachment occurs and eventually along all the subsequent trajectories steps, the process energy dissipation can be measured.

It should be noted that dissipation in AFM operation can be recognized and described in two different situations; one is at the nanoscale level [11, 30] and the other one is at the atomic level [28, 29]. In the first case attention is concentrated on the relationship between energy dissipation and material properties such as surface adhesion energy and elastic properties [31, 32]. In the other case, the transformation of mechanical energy is directly related to atomic or molecular rearrangement at the sample surface. Our experiment, dealing with the detachment of gold nanoclusters on silicon surfaces, clearly falls within the first category.

In this contribution we will present a successful application of this procedure to obtain controlled detachment of gold nanoclusters on silicon and to estimate the energy depinning threshold as a function of cluster size. The results of the experiment show unambiguously that the AM-AFM method and calibration procedure that we have used allow us to discern and measure the energy detachment threshold for cluster size down to the ten-nanometer scale.

More generally we believe that a systematic use of this method might help in understanding the dependence of adhesion and friction forces on the size of the nanocontact.

2. Sample preparation and experimental set-up

The gold nanoclusters were synthesized in a colloidal suspension starting from an aqueous solution of tetrachloroauric (III) acid hydrate ($HAuCl_4$, $3H_2O$). The procedure is described in detail elsewhere [27]. Two different sizes were selected, with nominal diameters 13 ± 2 nm (NP13) and 24 ± 4 nm (NP24), and the size distributions were checked by TEM (figure 1). Gold particles were deposited on clean silicon substrates (Si(100) + native oxide) by dipping the substrate into the solution (about 1 h) and then drying it with a nitrogen flux. The deposition then was checked by SEM (figure 2).

Experiments were performed in air, at room temperature using a commercial AFM microscope (Enviroscope + Nanoscope IV, by VEECO). The humidity during the experiments was about 40% and it was regularly monitored. Two different sets of standard silicon cantilevers have been used (Veeco RTESP5, RFESP), characterized by nominal frequencies $f_0 = 75$ and 350 kHz and spring constants K of 3 and 40 N m^{-1} respectively. The spring constant of each cantilever has been individually checked following the criterion of Sader *et al* [35]. The corrected K values were used during the energy calibration procedure to better compare measurements performed with different tips and to minimize non-systematic errors. However, small but systematic errors on the evaluation of K parameter may affect the absolute energy scale and they cannot be completely ruled out.

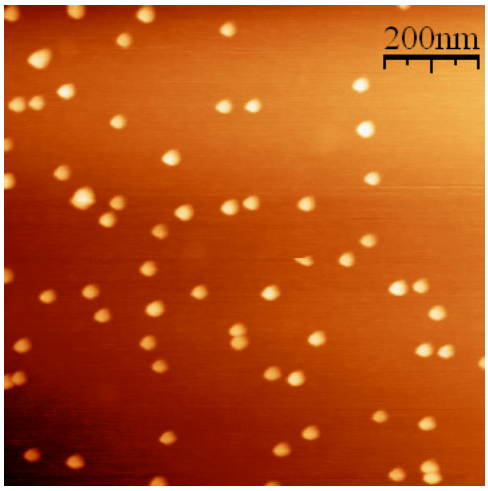

Figure 3. Deposition of nanoclusters with 13 nm nominal diameter (NP13) on clean SiO_2 (roughness 0.5 nm). Density: 65 particles over 1 μm^2. Topographic image, no filtering.

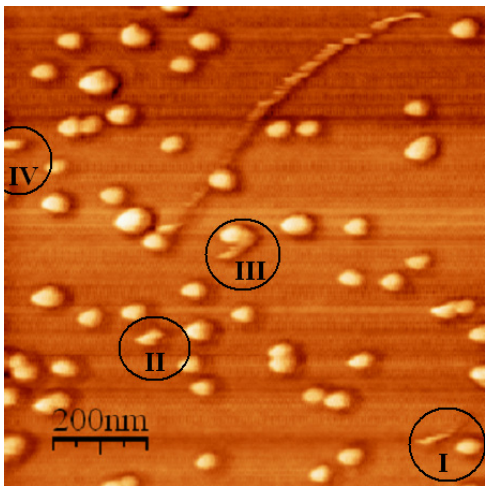

Figure 4. Phase contrast image during a typical *manipulation scan* over the same area as in figure 3. Marked zones are described in the text.

3. Experiment

A single manipulation measurement consists in taking a sequence of images of a selected area and a dedicated calibration procedure that allows one to correlate the phase shift signal with an energy measurement. Before going into the details of this procedure, let us describe the manipulation sequence. The AFM is used in tapping mode with amplitude feedback (AM-AFM) with a scan rate of 1 Hz and 512 sample/lines. During the sequence, we alternate a standard imaging scan and a *manipulation scan,* where the oscillation amplitude of the cantilever driving piezo is progressively increased with respect to the previous *manipulation scan*, keeping all the other AFM parameters unchanged. Above a certain oscillation amplitude, detachment events start to occur. The sequence usually ends when the number of detachment events between subsequent *manipulation scans* is close to zero. Representative image and *manipulation scans* are shown in figures 3 and 4, respectively.

Figure 3 represents a standard topographic image of an NP13 sample (nanoclusters with nominal diameter of 13 nm). Single nanoclusters are easily identified and the observed distribution of heights reflects correctly the diameter distribution obtained by TEM and SEM, confirming that clusters have nearly spherical shape. In contrast, the apparent diameter directly deduced from AFM images (∼25 nm in this case) always reveals a large influence of size of the tip.

Figure 4 displays a phase contrast image obtained during a typical *manipulation scan* over the same area as in figure 3 showing the details that characterize the cluster movement induced by the tip.

Some peculiar detachment events have been marked on figure 4: (I) the indication of a 'track' followed by a large displacement, moving the particle out of the field of view, (II) a small jump to the right with the particle remaining pinned in the new position, (III) a 'collision' between a moving particle and a pinned particle that traps the moving one, (IV) a detachment and a movement out of the field of view. But the more interesting feature present in this image is the evident 'track' which goes from the center to the upper right corner, consisting of a series of small jumps performed by a nanocluster after the first detachment. The particular direction of movement and the variability of jump length clearly show that tip does not drag the particle, but instead it forces scan by scan the movement along the slow scan direction (from bottom to top in this case). It is also evident that the preferred direction is related to the scan step and shape of the tip because tracks within the same scan or sequence are usually parallel to each other, while the substrate does not possess any particular symmetry. Moreover it should be noted that the phase shift signal associated with the small jumps that form the track are lightly smaller than the one related to the first detachment.

The comprehension of the intriguing effects described above requires a detailed description of the mechanisms controlling the tip–cluster dynamics. Nevertheless here we want to focus on the process of energy dissipation taking place at the very first stage of nanocluster detachment, with the aim of relating the depinning threshold and adhesion effects to the cluster size (i.e. to the contact area at the nanoscale).

To measure the energy threshold associated with a particle detachment we use the phase contrast method described in detail in recent publications [31–34]. The method relies on the description of the cantilever–tip system interacting with a surface as an externally driven anharmonic oscillator with damping. The external driver is the piezo oscillation at base of the beam, while the damping contribution comes from two distinct channels: the intrinsic one (air damping and beam deflection) and the tip–substrate interaction.

The measurable quantities associated with damping effects are frequency, amplitude and phase shifts. Using the microscope with amplitude feedback at fixed frequency, we force the system to show all the dissipation effects in the phase shift. At the resonant frequency, the energy dissipation per cycle due to tip–surface interaction E_{int} can be expressed as

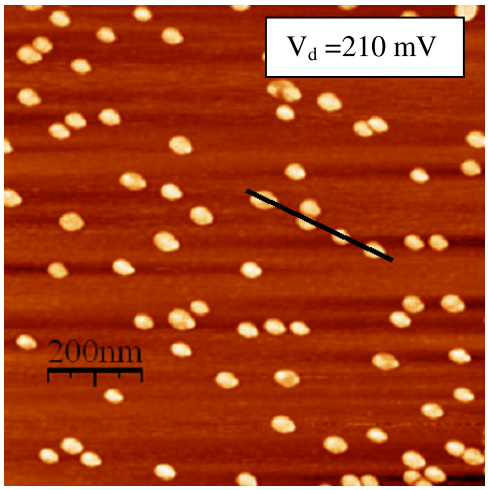

Figure 5. Phase image during a *manipulation scan*. The black line marks the direction corresponding to the line profile presented in figure 6 (right). V_d is the voltage applied to the cantilever driving piezo during the acquisition of this image.

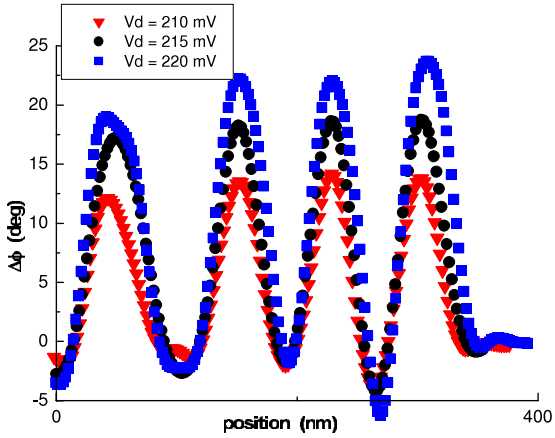

Figure 6. Phase shift deduced from phase images recorded at three different values of the cantilever driving piezo voltage (V_d). The profile follows the black line in figure 5 (left). The increase of phase shift is similar for all four clusters and directly depends on V_d.

follows [31]:

$$E_{\text{int}} = \frac{\pi k A}{Q}(A_0 \sin\phi - A) \tag{1}$$

where Q and k are, respectively, the quality factor and the spring constant of the cantilever, ϕ is the phase shift between the external driving oscillation and the tip response, A is the oscillation of the tip in contact with the surface (i.e. the amplitude set-point which is kept constant by the feedback loop), and A_0 is the tip free amplitude oscillation that we intentionally increase during a manipulation sequence.

Two important aspects have to be noted. First, at the resonant frequency, A_0 is a linear function of the external driving oscillation amplitude A_d, controlled by the applied voltage V_d. Second, A_0 and A have to be expressed in units of length. A calibration procedure is therefore associated with each manipulation sequence. It starts with the evaluation of the Q factor and of the curve V_0 versus V_d (V_0 is the photodiode measurement of A_0 and V_d is the voltage applied on the driving piezo), and it ends with the estimation of the deflection sensitivity which recasts photodiode measurements into units of length. Following this procedure, we are able to associate an energy value with each measured phase shift, taking into account the particular cantilever and microscope set-up.

4. Results and discussion

During a manipulation sequence, each increase of the driving oscillation amplitude produces a marked increase of phase shift localized on the nanoclusters. Within a given image, as shown in figures 5 and 6, the variation is similar for all the sampled clusters. For this reason we do not calculate the phase shift on each cluster; rather, for each driving oscillation amplitude, we evaluate the average phase shift over the whole set of nanoclusters, including also the moving ones. We have checked that the maximum error associated with this procedure is always smaller than the step induced by the driving oscillation increase and also, for different events where the phase shift is clearly visible before detachment (IV in figure 4), that no anomalous shift appears in these situations.

Finally, according to equation (1) and to the calibration procedure, we calculate a unique energy value from a couple of A_0 and ϕ measurements and we associate with that value the number of nanoclusters being eventually detached during the scan.

The results of this analysis for both NP13 and NP24 samples are shown in figure 7. The data represent the collection of a number of different manipulation sequences covering an equivalent area of 8 μm^2, counting about 400 (NP13) and 300 (NP24) nanoclusters. The left vertical axis refers to the histogram of detachment events. The right vertical axis refers to the curve representing the sum of the detachment events achieved up to an energy value E. Both representations are normalized to the total particle number.

The two histograms present similar behaviors, even if the distribution is broader for the larger cluster family (NP24). There is a gradual increase of the detachments probability for increasing energy dissipation up to a maximum, followed by a much faster decrease. This behavior is well described by the curve representing the incremental sum of the detachment events. The maximum is marked by the abrupt change of the curve slope at high energy and we use this indicator as a significant point for fixing the energy threshold values: $E_{13} = 6.9 \times 10^{-16}$ J (NP13), $E_{24} = 21 \times 10^{-16}$ J (NP24). We estimate the error bar associated with these values as equal to the width of the histogram column, $\Delta E = 2 \times 10^{-16}$ J.

The data summarized in figure 7 are the results of a well defined measurement procedure that has been controlled and repeated several times. In particular we want to emphasize that a number of different tips have been used, which correspond to different spring constants and resonant frequencies but also to a variety of tip shapes. These are typical parameters that may affect the quantitative comparison of AFM data. The

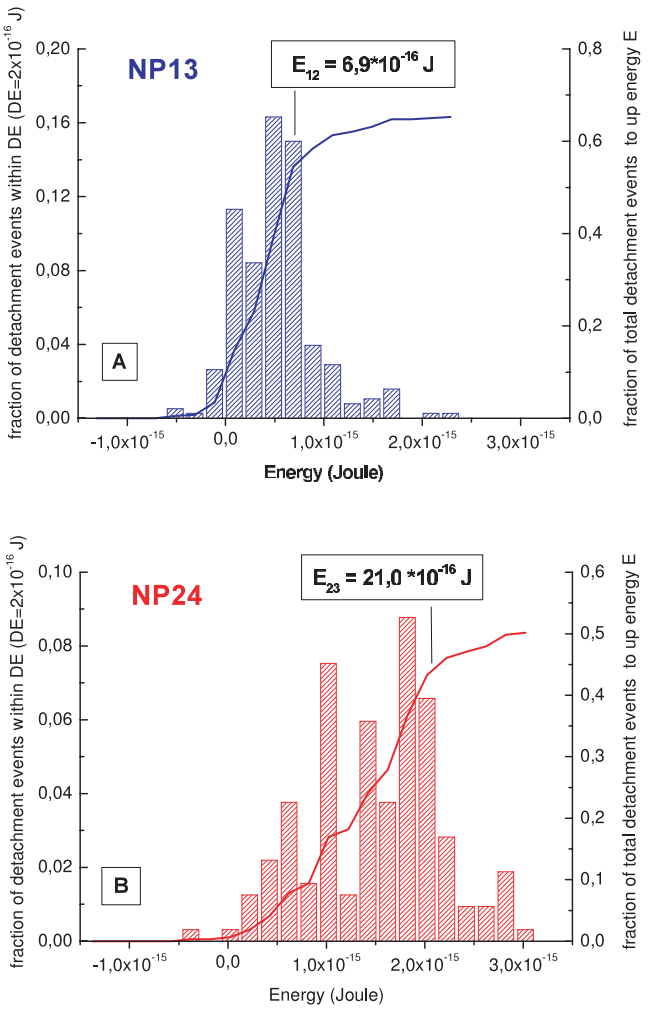

Figure 7. Data represent the collection of a number of different manipulation sequences covering an equivalent area of 8 μm^2, containing about 400 (NP13 (A)) and 300 (NP24 (B)) nanoclusters. The left axis refers to the histogram of detachment events. The right axis refers to the curve representing the sum of the detachment events achieved up to the energy E. Both representations are normalized to the total particle number and give clear evidence of the two separate energy detachment thresholds. The abrupt change of the slope in the curves is a significant point for fixing the energy threshold values: $E_{13} = 6.9 \times 10^{-16}$ J (NP13), $E_{24} = 21 \times 10^{-16}$ J (NP24). We estimate the error bar associated with these values as equal to the width of the histogram column, $\Delta E = 2 \times 10^{-16}$ J.

measurement and the statistical procedure that we have used allow us to account for these effects in such a way that data obtained for slightly different operational conditions can be properly compared and averaged together.

It has been experimentally shown recently that the adhesion energy of nanoclusters depends on their size down to a contact area of about 10^4 nm^2 [24]. Actually we have been able to give clear evidence of the separate energy detachment thresholds for cluster sizes down to the ten-nanometer range, which correspond to a contact area two orders of magnitude smaller than for previous results.

Finally, we can tentatively extrapolate a size dependent behavior from our results. The morphological characterization (TEM + SEM images and height distribution from AFM) confirm that our clusters have a nearly spherical shape. Within a continuum description and following the above approximation, the contact area should be, in any case, proportional to the projected area of the cluster on the surface calculated from its nominal diameter. The variation of the projected area from small to large clusters is by about a factor of 3.4. The ratio of the energy detachment data, going from the smaller to the larger clusters, is consistent with the assumption of a direct proportion between the contact area and energy depinning threshold.

5. Conclusion

The data presented show unambiguously that the AM-AFM method and the calibration procedure that we have described allow us to discern and measure the energy detachment threshold for cluster size down to the ten-nanometer scale. The results are in qualitative agreement with [24] but they represent a step forward in the direction of measuring and controlling nanometer mechanical properties. Finally the method proves to be a valuable tool for nanomanipulation purposes, since it allows one to switch easily and with high repeatability between imaging and manipulation scans during AFM measurements.

Acknowledgments

The authors like to thank Dr G C Gazzadi for the SEM images. This research was partially supported by PRRIITT (Regione Emilia Romagna), Net-Lab 'Superfici & Ricoprimenti per la Meccanica Avanzata e la Nanomeccanica' (SUP&RMAN).

References

[1] Mate C M, McClelland G M, Erlandsson R and Chiang S 1987 *Phys. Rev. Lett.* **59** 1942
[2] Fujisawa S, Kishi E, Sugawara Y and Morita S 1995 *Phys. Rev.* B **51** 7849
[3] Schwarz U D, Köster P and Wiesendanger R 1996 *Rev. Sci. Instrum.* **67** 2560
[4] Bennewitz R, Gyalog T, Guggisberg M, Bammerlin M, Meyer E and Güntherodt H-J 1999 *Phys. Rev.* B **60** R11301
[5] Urbakh M, Klafter J, Gourdon D and Israelachvili J 2004 *Nature* **430** 525
[6] Socoliuc A, Bennewitz R, Gnecco E and Meyer E 2004 *Phys. Rev. Lett.* **92** 134301
[7] Dienwiebel M, Verhoeven G S, Pradeep N, Frenken J W M, Heimberg J A and Zandbergen H W 2004 *Phys. Rev. Lett.* **92** 126101
[8] Bennevitz R 2005 *Mater. Today* **8** 42
[9] Gnecco E and Meyer E (ed) 2006 *Fundamentals of Friction and Wear on the Nanoscale* (Berlin: Springer)
[10] Sugimoto Y, Jelinek P, Pou P, Abe M, Morita S, Perez R and Custance O 2007 *Phys. Rev. Lett.* **98** 106104
[11] Falvo M R, Taylor R M, Helser A, Chi V, Brooks F P Jr, Washburn S and Superfine R 1999 *Nature* **397** 236
[12] Lüthi R, Meyer E, Haefke H, Howald L, Gutmannsbauer W and Güntherodt H-J 1994 *Science* **266** 1979
[13] Adams D M *et al* 2003 *J. Phys. Chem.* B **107** 6668
[14] Haruta M 2002 *CATTECH* **6** 102
[15] Valden M, Lai X and Goodman D W 1998 *Science* **281** 1647
[16] Wang J 2003 *Anal. Chim. Acta* **500** 247
[17] Penn S G, He L and Natan M J 2003 *Curr. Opin. Chem. Biol.* **7** 609

[18] Heinrich A J, Lutz C P, Gupta J A and Eigler D M 2002 *Science* **298** 1381
[19] Nazin G V, Qiu X H and Ho W 2003 *Science* **302** 77
[20] Cuberes M T, Schlitter R R and Gimzewski J K 1996 *Appl. Phys. Lett.* **69** 3016
[21] Butcher M J, Nolan J W, Hunt M R C, Beton P H, Dunsch L, Kuran P, Georgi P and Dennis T J S 2003 *Phys. Rev.* B **67** 125413
[22] Junno T, Deppert K, Montelius L and Samuelson L 1995 *Appl. Phys. Lett.* **66** 3627
[23] Hsieh S, Meltzer S, Wang C R C, Requicha A A G, Thompson M E and Koel B E 2002 *J. Phys. Chem.* B **106** 231
[24] Ritter C, Heyde M, Stegemann B and Rademann K 2005 *Phys. Rev.* B **71** 085405
[25] Aruliah D A, Muser M H and Schwarz U D 2005 *Phys. Rev.* B **71** 085406
[26] Ritter C, Heyde M, Schwarz U D and Rademann K 2002 *Langmuir* **18** 7798
[27] Mougin K, Gnecco E, Rao A, Cuberes M T, Jayaraman S, McFarland E W, Hairada H and Meyer E 2008 *Langmuir* **24** 1577
[28] Trevethan T, Watkins M, Kantorovich L N and Shlugher A L 2007 *Phys. Rev. Lett.* **98** 028101
[29] Sugimoto Y, Pou P, Abe M, Jelinek P, Perez R, Morita S and Custance O 2007 *Nature* **446** 64
[30] Gotsmann B, Seidel C, Anczykowski B and Fuchs H 1999 *Phys. Rev.* B **60** 11051
[31] Garcia R, Gomez C J, Martinez N F, Patil S, Dietz C and Magerle R 2006 *Phys. Rev. Lett.* **97** 016103
[32] Garcia R, Magerle R and Perez R 2007 *Nat. Mater.* **6** 405
[33] Anczykowski B, Gotsmann B, Fuchs H, Cleveland J P and Elings V B 1999 *Appl. Surf. Sci.* **140** 376
[34] Cleveland J P, Anczykowski B, Schmid A E and Elings V B 1998 *Appl. Phys. Lett.* **72** 2613
[35] Sader J E, Chon J W M and Mulvaney P 1999 *Rev. Sci. Instrum.* **70** 3967–9